Angle-resolved photoemission determination of the band structure of Ru(001)

M. Lindroos,* P. Hofmann, and D. Menzel
Fakultät für Physik (E20), Technische Universität München, D-8046 Garching bei München, West Germany
(Received 4 October 1985)

Synchrotron radiation in the energy range from 11 to 80 eV has been used to identify critical points in the Ru band structure along ⟨001⟩ and to map the energies of the electronic states. The experimental band structure is compared to various theoretical calculations. We find good agreement between experiment and calculations using the proper hcp symmetry for the occupied bands. Peaks in the photoemission spectra not related to direct bulk transitions are attributed to surface states or resonances (i.e., a part of the peak in the vicinity of E_F and a peak at $E_B=-5.6$ eV), and to two-electron excitations (at a binding energy E_B of ≈ -7.3 eV, in coincidence with a one-electron band-structure state) which are resonantly enhanced at the Ru $4p$ core level. Another prominent peak in the spectra at fixed kinetic energy of ≈ 16.5 eV relative to E_F must be attributed to emission into a flat final band. The interpretations are supported by theoretical calculations of the photoemission intensities. The calculations are based on the one-step model of the photoemission process.

I. INTRODUCTION

The recent availability of synchrotron radiation has prompted many experimental energy-band dispersion studies using Angle-resolved ultraviolet photoemission spectroscopy (ARUPS).[1,2] It is a rather straightforward procedure to evaluate normal-emission spectra if a free-electron-like final-state band can be used. Dangerous pitfalls can be avoided by the use of tunable radiation which makes it possible to distinguish between initial- and final-state peaks. In this respect we note that a strong peak, which is found at an apparent binding energy of $E_B=-4.5$ eV in He I spectra from Ru, is, in fact, a final-state peak at fixed kinetic energy equal to 16.5 eV. Without variable photon energy this peak could be mistaken as an occupied band feature.

Nickel and copper have become the prototype transition metals for ARUPS, both experimentally and theoretically.[3–5] While there is very good agreement between theory and experiment for Cu, even if simple free-electron-like final bands are used, there are substantial discrepancies for Ni. This is thought to be due to the strong localization of the d bands in Ni, which shows up as a d-band narrowing coupled with strong multielectron excitations.[3]

Investigations of metals with hexagonal-close-packed (hcp) structure are still rare, although the hcp structure is the most common among the transition metals. Experimentally, Himpsel and Eastman have investigated Co(001) and have found good agreement between experiment and a self-consistent calculation for Co.[6] Himpsel *et al.*[7] have also studied the band dispersion of Ru along the ⟨001⟩ axis using photoelectron spectroscopy, but the agreement with two bulk electronic band-structure calculations[8,9] available at that time was not so good. Experimentally, the present results are rather similar to those of Himpsel *et al.*[7] Our larger data base and the theoretical intensity calculations, however, allow a more detailed evaluation of the spectra which leads to some significant differences in interpretation of the origin of the spectral features. Very recently, Heskett *et al.*[10] have studied adsorption of CO and N_2 on Ru(001) and they also present some results for clean ruthenium.

The present study has been initiated by our interest in the adsorption of various "simple" adsorbates such as H_2, CO, NO, and N_2O on Ru (Refs. 13–15). In order to study two-dimensional adsorbate states, at first the bulk band structure needs to be known. Furthermore, some new band-structure calculations for Ru in addition to ours have just become available, which allow more detailed comparisons between experiment and theory. We are also interested in the extent of the applicability of the calculations based on the one-step model to describe the photoemission process.[16]

At present there are at least six different band-structure calculations available for Ru (Refs. 8, 9, 17, and 18) (Fig. 7). The modified augmented-plane-wave[18] calculations of Bross and Krieter made use of the crystal potential of Moruzzi *et al.*,[9] whose own band-structure calculations were done for pseudo-fcc Ru. The band structure of Ref. 17 has been calculated using an APW, while Jepsen *et al.*[8] used a relativistic linear muffin-tin orbital calculation. In the latter case spin-orbit coupling leads to splitting of the bands. This theory indicates that this effect is still small for Ru. Recently, Holzwarth *et al.*[19] have derived the electronic structure of Ru using *ab initio* pseudopotentials and a mixed basis. In this and also in Feibelman's work[20] the surface electronic structure of Ru is presented.

On the other hand, there seems to be only one published calculation of the intensities of ARUPS within hcp crystal structure.[21] A computer code, PEOVER, for calculating the angle-resolved photocurrent within the one-step model, has been developed by Hopkinson *et al.*[11] Larsson[12] has extended this computer program to include ordered binary compounds and multilayer structures. With this new version, NEWPOOL, the hexagonal crystal structure can be studied as a special case, taking the component atoms as identical.

In the next section we describe the experimental setup

and the procedure to derive $E(\mathbf{k})$ dispersion relations from experimental results. In Sec. III we introduce the theoretical background of our intensity and band-structure calculations. In Sec. IV we introduce our theoretical band structure of Ru (001) in order to help the reader to follow our interpretations of our experimental results (Sec. V). In Secs. VI and VII we discuss multielectron excitations and two-dimensional states and, finally, compare experimental and theoretical band structures.

II. EXPERIMENT AND PROCEDURE

The experiments were performed at the Berlin storage ring for synchrotron radiation [Berliner Elektronenspeicherring-Gesellschaft für Synchrotronstrahlung (BESSY)], using a toroidal-grating monochromator (TGM 2) coupled to an angle-resolved photoelectron spectrometer (ADES 400, Vacuum Generators). The angular acceptance was $\approx \pm 1°$ and the combined resolution of the monochromator and the analyzer was set at typically 200 meV (Ref. 22).

The Ru (001) crystal, oriented and precleaned as described elsewhere,[13] was cleaned *in situ* using oxygen treatment and subsequent flashing in vacuum to 1560 K. The background pressure in the ultrahigh-vacuum (UHV) chamber was $<2\times10^{-10}$ Torr. Ordering and cleanliness were checked with low-energy electron-diffraction (LEED), Auger-electron spectroscopy (AES), and thermal-desorption spectroscopy (TDS) experiments. The crystal could be cooled to ≈ 200 K and was mounted in such a way that off-normal experiments could be performed along $\bar{\Gamma}\bar{K}$ with the detector in the plane of incidence of light and along $\bar{\Gamma}\bar{M}$ with the detector perpendicular to the plane of incidence. The polar angle of incidence, α, could be varied independently from the electron-emission polar angle θ. Both angles are measured with respect to the surface normal.

The experimental data have been analyzed using the direct-transition model. For determining a component of $\mathbf{k}$ along $\langle 001 \rangle$, $k_\perp$, we have utilized the following semiempirical method, which has been successfully applied to many metals.[1,2] At first we determine, in normal emission, critical points of the final-state bands, which show up as extremal behavior (with respect to intensity and/or peak positions) of experimental peaks, and as structures in the spectra of secondary electrons. Secondly, a free-electron-like parabola is interpolated between the obtained critical points. The energy difference between the minimum of the parabola and the vacuum level is an experimental inner potential. Thirdly, $k_\perp$ is obtained from the observed final energy via the E_f-vs-$k_\perp$ dispersion of the final bands.[1,2] It has been shown that this procedure introduces only minor errors in $k_\perp$ ($\approx 10\%$) and negligible errors for the initial energy in the flat d-band region. The procedure is mostly used for normal emission, when $k_\parallel$, the component of $\mathbf{k}$ parallel to the surface, is equal to 0. We have also collected some off-normal data which have been analyzed using a procedure as described, e.g., by Eberhardt and Plummer,[2] using *free-electron* final bands. $\mathbf{k}$ is then given by

$$k_\perp = \frac{1}{\hbar} \left| 2m^*(E+V_0) - \hbar k_\parallel^2 \right|^{1/2} \tag{1}$$

and

$$k_\parallel = \frac{1}{\hbar}(2m^*E)^{1/2}\sin\theta \, . \tag{2}$$

In these equations E_K is the kinetic energy of the emitted electron, V_0 is the experimental inner potential, and m^* is the effective electron mass, which is, as in this study, usually taken equal to the free-electron mass.

Finally, we would like to point out the similarity between the hcp (0001) and fcc (111) close-packed crystal structures. The line $\Gamma\Delta A\Delta\Gamma$ in the hcp Brillouin zone (BZ) corresponds to the line $\Gamma\Lambda L$ in the fcc BZ. Here we will use this double-zone scheme, with $\Gamma\Delta A\Delta\Gamma$ as a basic unit, to represent the experimental band structure in Figs. 12 and 14 for clarity. The advantage of this double-zone scheme is that the number of electron bands is reduced by a factor of 2 (Refs. 6 and 8).

III. THEORY

According to Caroli *et al.*,[23] the photocurrent in the photoemission process can be obtained from the formula

$$I(k_\parallel, E+h\nu) = -(1/\pi)\,\mathrm{Im}[\langle\phi \,|\, G_2^+(E+h\nu)\Delta G_1^+(E)\Delta^\dagger G_2^-(E+h\nu) \,|\, \phi\rangle] \, . \tag{3}$$

In this equation the Green's functions $G_2^\pm$ and G_1^+ describe the propagation of electron and hole, respectively. Δ and $\Delta^\dagger$ are perturbing terms in the Hamiltonian due to the photon field, i.e.,

$$\Delta \approx \mathbf{p}\cdot\mathbf{A} + \mathbf{A}\cdot\mathbf{p} \, . \tag{4}$$

Equation (3) is the starting point of Pendry's[24] formulation of the angle-resolved photoemission process. Equation (3) is solved by the computer code of Hopkinson *et al.*,[11] in which the crystal structure and the potential are provided as input. In this computer program the photoemission from a single atom is calculated to first order in the photon field. No energy dependence of the optical constants is taken into account, which complicates direct comparison between theoretical and experimental intensities. The initial- and final-state corrections are made by calculating multiple scattering *within* and *between* the layers of the crystal. The crystal is described by stacking atomic layers and the crystal potential is assumed to have a muffin-tin form.

Although band structure is not directly used in photoemission calculations, it may be extracted from the quantities that are calculated by the PEOVER or NEWPOOL pro-

grams.[11] The wave function, traveling in the $\pm z$ direction (normal to the crystal surface) between the jth and the $(j+1)$th atomic layers, is represented as

$$\phi_j^{\pm}=\Sigma_{\mathbf{g}} a_{\mathbf{g}}^{\pm} e^{\pm i\mathbf{K}_{\mathbf{g}}\cdot(\mathbf{r}-\mathbf{c})} . \tag{5}$$

$\mathbf{g}$ are the two-dimensional reciprocal-lattice vectors and $\mathbf{c}$ is the translation vector from the origin of one atomic layer to another. $a_{\mathbf{g}}^{\pm}$ are the amplitudes of each plane wave. We can write

$$\begin{bmatrix} I & -R \\ 0 & P^- T \end{bmatrix} \begin{bmatrix} \phi_{j+1}^+ \\ \phi_{j+1}^- \end{bmatrix} = \begin{bmatrix} TP^+ & 0 \\ -P^- RP^+ & I \end{bmatrix} \begin{bmatrix} \phi_j^+ \\ \phi_j^- \end{bmatrix} , \tag{6}$$

where R is the reflection matrix of the atomic layer, T the transmission matrix, and

$$P_{\mathbf{gg}}^{\pm}=e^{\pm i\mathbf{K}_{\mathbf{g}}\cdot(\mathbf{c}_{j+1}-\mathbf{c}_j)} \tag{7}$$

are propagators from one layer to the next, and

$$\mathbf{K}_{\mathbf{g}}=(\mathbf{k}_{||}+\mathbf{g}, k_{\perp}) , \tag{8}$$

where $\mathbf{k}_{||}$ and $k_{\perp}$ are the components of the $\mathbf{k}$ vector of the emitted electrons in Eqs. (1) and (2).

According to Bloch's theorem,

$$\phi_{j+1}=e^{i\mathbf{k}\cdot\mathbf{c}}\phi_j , \tag{9}$$

which defines, together with Eq. (6), a general eigenvalue problem to be solved by standard methods.

In our calculations tabulated crystal-potential values of Moruzzi *et al.*[9] were used as input. As a self-energy correction for the crystal potential of the excited state, a complex optical potential was introduced. The real part of the inner potential, i.e., the energy distance between the vacuum level and the muffin-tin zero of the crystal potential, was chosen to be 14 eV. The exact value of V_0 could be extracted from off-normal data via Eqs. (1) and (2). This analysis, however, is complicated by the two domains present, so we have just adopted this value, which is, according to our experience, reasonable. The (negative) imaginary part of the optical potential, $V_{o,i}$, for holes, was set to 0.5 eV, as this value gives correct widths of the peaks. In the present calculation we have not made $V_{o,i}$ go to zero at E_F, as is physically required. This does not appear to be important here, as the total peak width will be given by the convolution of initial- and final-state widths, and the latter will remain considerable. For electrons we used a rather small value of 1 eV based on our study of the 16.5-eV final-state feature,[25] although the value of this parameter is not critical for the present study. In the band-structure calculations a value of 0.005 eV was used for both holes and electrons. This is because band-structure calculations are generally done with an imaginary part of the optical potential equal to zero.

To facilitate the comparison between experimental and theoretical spectra (see Figs. 2–5), a smooth secondary-electron distribution has been added to the theoretical spectra. This background has been successfully described by the function[26]

$$f(E)=C(E-\phi)/E^4 , \tag{10}$$

where ϕ is the work function, for which we used a value of 5.4 eV. The energy E is measured with respect to the Fermi level. C is the intensity normalization constant, for which we used a value of 2 times the maximum peak intensity of the spectrum.

The influence of the Fermi level has been described by multiplying the intensity as obtained above by

$$g(E)=\frac{1}{1+e^{E/kT}} . \tag{11}$$

To mimic the broadening of the experimental Fermi-edge structures due to the resolution of the instrument, we have used an unphysically high value of 0.1 eV for kT in our calculation. The same spectral effect could be obtained by using the proper value for kT and then convoluting the spectra with a Gaussian function having a width of 0.1 eV. The additional broadening of all structures due to this convolution would have to be taken into account when a value of $V_{o,i}$ is determined.

IV. THEORETICAL BAND STRUCTURE

Before presenting any detailed considerations of the experimental and theoretical results, we want to show for clarity our theoretical band structure of Ru(001) in Fig. 1. We have obtained the bands using the layer method described in the preceding section. In practice, the calculations of the matrices in Eq. (6) are performed at fixed energy. From Eqs. (6) and (9) we then obtain possible $k_{\perp}$ values, complex due to the complex optical potential. The solid lines in Fig. 1 correspond to those $E(k_{\perp})$ points, whose $\mathrm{Im}k_{\perp}$ is small or zero. These bands can be identified with bands having only a real optical potential (or self-energy) and they should be compared with the results of the other band-structure calculations (see, e.g., Fig. 12 below).

There are also solutions of Eq. (9) in the gaps of the above bands. The important point now is that $\mathrm{Im}k_{\perp}$ is not zero any longer (or a small number). These gap bands are sensitive to the imaginary part of the optical potential, $V_{o,i}$. When $V_{o,i}$ is small (0.005 eV), $\mathrm{Im}k_{\perp}$ in the gap is large (0.5) compared to $\mathrm{Im}k_{\perp}$ of the "real" band (0.001 or less). However, when $V_{o,i}$ is increased, $\mathrm{Im}k_{\perp}$ of the "real" band increases. When $V_{o,i}$ is relatively large, say 4 eV, the difference between $\mathrm{Im}k_{\perp}$ of the "real" and the gap band is insignificant and we have continuous free-electron-like bands.

As mentioned above, we have performed our intensity calculations using $V_{o,i}=1$ eV. Our $E(k_{\perp})$ band of the photoemission final state is shown in Fig. 1 as a dashed line, even in the gaps, where $\mathrm{Im}k_{\perp}$ is large. This band is very important, as it gives rise to the position of the peaks in our theoretical photoemission spectra. Energy positions of most peaks are determined by the crossing points of this final-state band with the initial-state bands in Fig. 1. Figure 1 also shows why we might have poor agreement even if our band structure is very accurate, but calculated with the real optical potential. It clearly demonstrates why free-electron final states, displayed as dotted lines, give a much better description: The difference between energies of the free-electron final state and the finite $V_{o,i}$ final state is smaller than the difference between

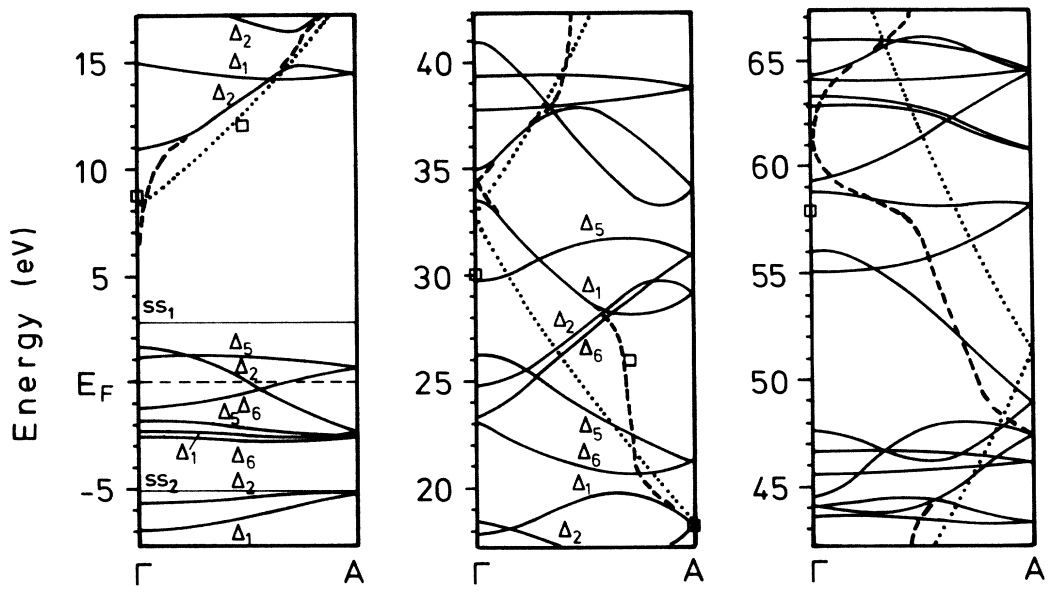

FIG. 1. Calculated initial- and final-state bands for Ru(001) along ΓA. Dots correspond to free-electron-like final-state bands fitted to the critical points marked with squares. Dashed lines present photoemission final-state bands. SS_1 and SS_2 refer to Shockley-type surface states.

the zero $V_{o,i}$ band and the nonzero $V_{o,i}$ band due to continuation of the bands in the gaps.

There are some other consequences of the shape of the final-state band. In the energy range of the band gap its slope is rather steep, at least significantly steeper than in the nongap case. In the case of small $V_{o,i}$ it is steeper than it is with larger $V_{o,i}$. This behavior has two consequences. In the first case the absolute intensity of the gap states is small, which is reasonable, because the density of final states is small. When $V_{o,i}$ is larger, we have larger intensity from the gap states caused by higher density of states due to a more gentle sloping or, in other words, due to a smearing and broadening of the bands.

The latter effects are also obvious in Fig. 1: In the gap $k_\perp$ does not change much, when the energy of the final state is changed over the gap. This means that the energy positions of the peaks in photoemission spectra do not change, when the photon (and thus the final-state) energy is swept over the gap. (See, e.g., Fig. 13, with a photon energy range from 20 to 28 eV.)

V. EXPERIMENTAL BANDS AND CRITICAL POINTS

In Figs. 2 and 3 we show some selected experimental spectra in normal emission, and in Figs. 4 and 5 theoretical spectra corresponding to the same photon energies. We classify the spectral features following Himpsel *et al.*,[7] with emphasis on differences between their results and the present work.

(1) We have a spectral structure at $\approx E_F$ for $h\nu \approx 19$–28 eV. It becomes visible at $h\nu = 19$ eV, staying at constant energy of $E_B = -0.3$ eV for $h\nu = 22$–27 eV. In the latter range it is suppressed by adsorption of small

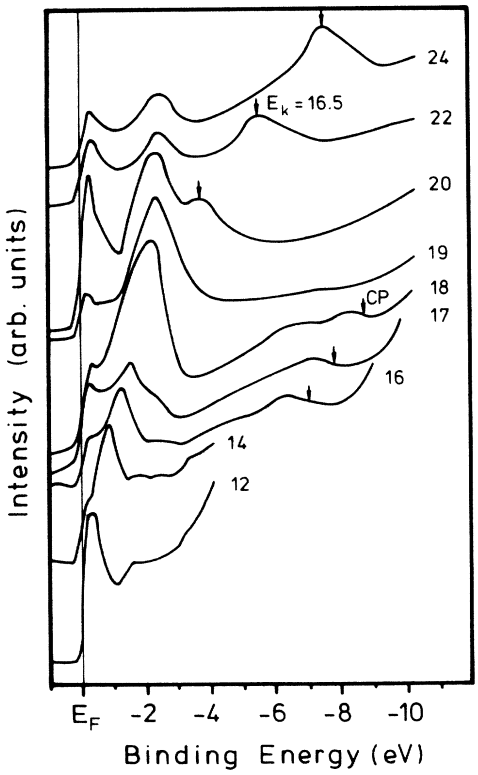

FIG. 2. Experimental photoemission spectra excited by p-polarized light in normal emission from clean Ru(001) for photon energies from 12 to 24 eV. Numbers refer to photon energies in eV. The first critical point, CP, is pointed out, as is the 16.5-eV final-state peak.

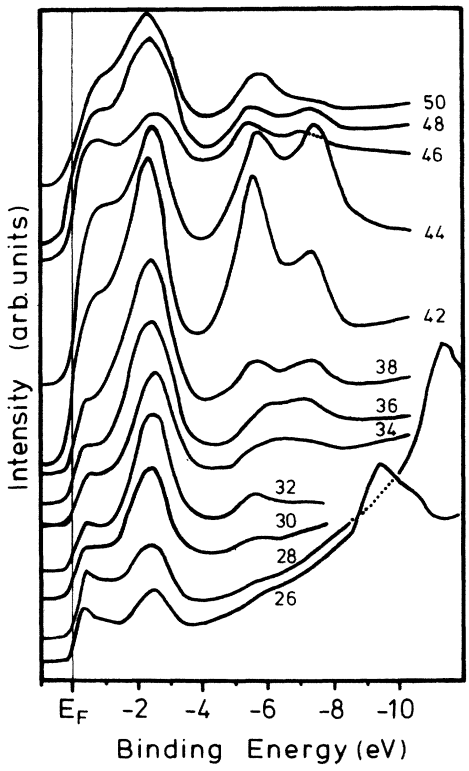

FIG. 3. Same as Fig. 2 for higher photon energies.

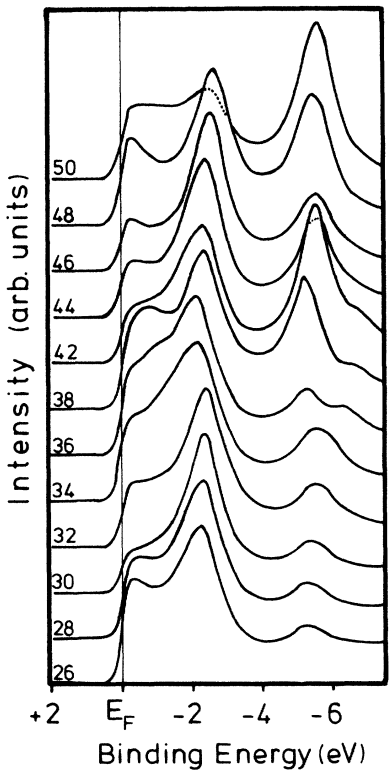

FIG. 5. Same as Fig. 4 for higher photon energies up to 50 eV.

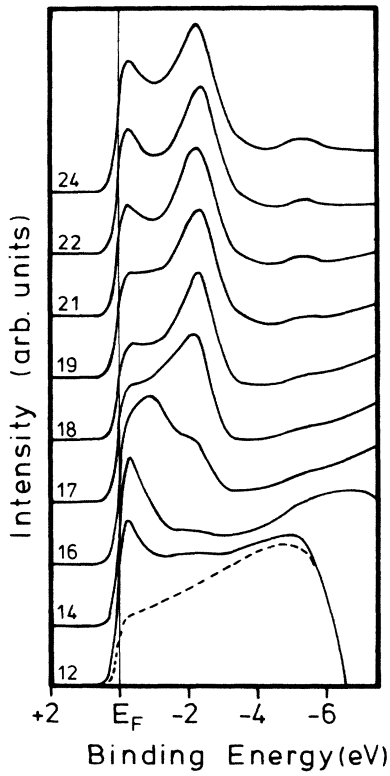

FIG. 4. Theoretical photoemission spectra corresponding to the same setup as in Fig. 2. Numbers refer to photon energies in eV. Dashed line displays background [product of Eqs. (10) and (11)] for $h\nu = 12$ eV.

amounts of CO, H, or O, and a second smaller peak or shoulder is more clearly visible than in the clean spectra.

The second structure disperses with $h\nu$ in the range mentioned above from ≈ -0.3 to -1.2 eV. This dispersive structure is visible *again* for $h\nu \approx 35$–44 eV, with opposite dispersion for increasing $h\nu$ (see Fig. 13). This peak can be seen when the light is incident near normal to the crystal surface (spectra not shown). We attribute this structure to the uppermost d band, Δ_6. The peak at constant $E_B = -0.3$ eV is due to "tails" of the possible peaks (d bands and a surface state; see discussion below) above the Fermi energy in the following sense. Both initial and final states have finite widths, and δ functions describing energy conservations must be replaced by proper spectral functions. For one initial band we can approximate the photoemission intensity as

$$I(E) \propto |M|^2 \times \int dk_\perp \frac{\Gamma_h(E_i(k_\perp))}{[E_i(k_\perp)-E]^2+[\Gamma(E_i(k_\perp))]^2} \times \frac{\Gamma_e(E_f(k_\perp))}{[E_f(k_\perp)-E_i(k_\perp)-h\nu]^2+[\Gamma_e(E_f(k_\perp))]^2}, \quad (12)$$

where M includes all matrix elements. If $E_i(k_\perp)$ crosses the Fermi level, like band Δ_6 in Fig. 1, we can divide $I(E)$

into two contributions, namely, into $I_>(E)$ if $E_i > E_F$ and into $I_<(E)$ if $E_i < E_F$. By calculating $I_>$ and $I_<$ from Eq. (12) by assuming that $\Gamma_h(E)=\alpha(E-E_F)^2$, $\Gamma_e=1$ eV, and $h\nu=24$ eV, we find that the main contribution of $I(E)$ below the Fermi level comes from $I_<(E)$, i.e., from lifetime broadening of the final states. However, at $E=E_F$ we have a small contribution from $I_>(E)$, which quickly dies away when we move lower below the Fermi level. So when we speak of the "tail" of the peaks above the Fermi level, we mean that for δ-function–type bands the peak might stay above the Fermi level, but due to broadening of the initial and final states we have contributions also below the Fermi level. As mentioned, we have used a constant $V_{o,i}$, and for $h\nu=24$ eV and the "−0.3-eV" peak we have $I_>$ and $I_<$ equal at E_F.

(2) A set of (usually unresolved) peaks at ≈ -2.4 eV binding energy represent the lower *d* bands, Δ_5 and Δ_6, and the upper *sp* band, Δ_1 (and Δ_2). By varying the angle of incidence α, we can study the symmetry of the initial states. When α is varied, the magnitude of the vector potential of light normal to the surface, A_z, is varied relative to the parallel components A_x and A_y. For *p* polarization and near-normal incidence (α small) we are exciting electrons by A_x or A_y depending on the azimuthal angle of incident light. For grazing incidence (α near 90°) electrons are excited by A_z. We can then use dipole selection rules to determine the symmetry of initial states. At first, we notice that the parity of the final state has to be even with respect to mirror planes. This means that possible final states are Δ_1 and Δ_2. Allowed interband transitions for the hcp (001) direction are given in Table I (Δ_3 and Δ_4 bands are not present).[6] In the table *s* means that emission excited by A_x or A_y is allowed. With *p*-polarized light we have two components A_z, and A_x or A_y. This second component A_x or A_y means that we have the same transitions present in the spectra excited by *p*-polarized light as are excited by *s*-polarized light. In the spectra excited by *p*-polarized light we also have contributions excited by A_z.

With *p*-polarized light and $\alpha=75°$, the peak maximum around Γ is found at −2.45 eV; for small α ($\alpha=20°$ and 45°) the peak is broader and some spectra allow the separation of two peaks at $E_B=-2.10$ and −2.75 eV. We associate the −2.45-eV peak with the Δ_1 band, the −2.10-eV peak with the Δ_5 band, and the −2.75-eV peak with the Δ_6 band.

(3) A peak at a constant final energy of 16.5 eV is associated with emission into a "flat" final-state band. Such a peak can also be excited by electrons.[27] This peak is particularly sensitive to adsorbates as reported in an earlier paper.[15] Similar final-state features, although much less prominent, have been found for various transition metals in normal emission.[3,6,28–30] In the case of Ru this peak is asymmetric with a main shoulder at $E_K \approx 16.5$ eV and a second weaker shoulder at ≈ 18 eV. It is resonantly enhanced at $h\nu \approx 19$ eV, where it coincides with the lower *d* band. This enhancement amounts to a factor of 2–3 compared to just the addition of both intensities, in agreement with the observations of Himpsel *et al.*[7] A detailed study of the origin of this spectral feature will be presented elsewhere.[25]

(4) The peak which rapidly disperses upward below $h\nu \approx 18$ eV (from E_F to ≈ -2 eV) with increasing $h\nu$ is attributed to the *sp* band, Δ_2, hybridized with the *d* band.

(5) The peak at ≈ -7.3 eV is seen from around $h\nu=32$ eV, in agreement with Ref. 7. It is, however, strongly enhanced at the Ru 4*p* core-level threshold at $h\nu=43$ eV ($4p_{3/2}$) and $h\nu=46$ eV ($4p_{1/2}$), respectively. This points to a multielectron satellite peak and contradicts Himpsel *et al.*,[7] who did not find this resonant enhancement at the core-level threshold. Their Fig. 2, however, indicates that the −7.3-eV peak is more intense at $h\nu=40$ eV than at $h\nu=37$ eV, in agreement with our data but in contradiction to their own interpretation. Their next spectrum shown is for $h\nu=50$ eV; at this photon energy the satellite peak is indeed practically no longer visible, as shown in our Fig. 8. The satellite masks the lower *sp* band in the vicinity of $h\nu=45$ eV. The intensity maximum at $h\nu=37$ eV of the −7.3-eV peak is attributed to a critical point in the Ru band structure. In our theoretical calculations we cannot, within our model, reproduce structures due to multielectron excitations. For further discussion, see Sec. VI below.

(6) The structure at −5.6 eV is associated with the flat, *d*-like section of the lowest band. The ordinary bulk band-structure calculation produces two bands, Δ_1 and Δ_2, at that energy range. Thus, in photoemission we would usually expect one peak and, in some rare occasions (near Γ), two peaks. The persistence of the peak at almost constant energy at all photon energies disagrees with the calculated band structure, i.e., with an interpretation that this peak is due to direct transitions only from Δ_1 and Δ_2 bands. We can, however, interpret the observed structures as a transition from a surface state *and* as direct transitions from Δ_1 and Δ_2 to available final states (see discussion of surface states).

In Fig. 6 we show a set of spectra with $h\nu=38$ eV as a function of the electron-emission angle θ. This figure clearly shows that only 10° off normal there are three components for the spectral structure 2. As mentioned, this analysis is complicated by the two domains present in the experimental spectra. To demonstrate the complications, we show in Fig. 7 theoretical spectra corresponding to the same photon energy and an electron emission angle of 10° toward $\bar{\Gamma}\bar{M}$ and $\bar{\Gamma}\bar{K}$. For $\bar{\Gamma}\bar{M}$, both domain contributions and their sum are displayed. For $\bar{\Gamma}\bar{K}$, contributions are equal and only one curve is shown in Fig. 7(c) (dashed line).

The critical points shown in Fig. 1 are determined as follows. The point at 8.7 eV at Γ is seen as a weak step

TABLE I. Allowed transitions of hexagonal (001) crystal structure due to dipole selection rules (Ref. 6).

	Δ_1	Δ_2	Δ_5	Δ_6
Δ_1	A_z			s
Δ_2		A_z	s	
Δ_5		s	A_z	s
Δ_6	s		s	A_z

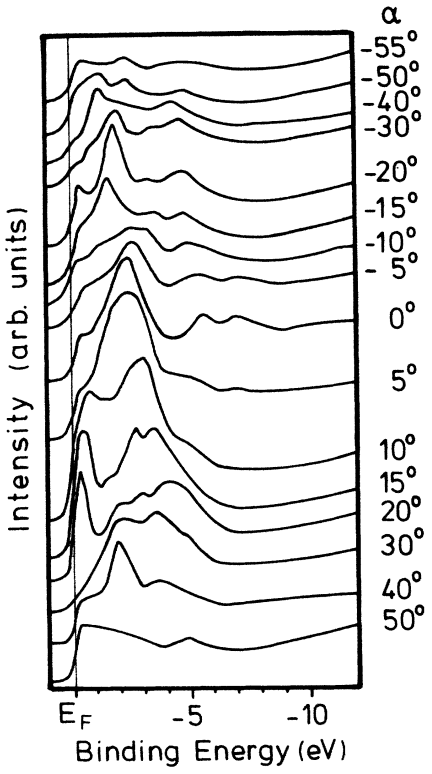

FIG. 6. Experimental off-normal photoemission spectra of Ru along $\bar{\Gamma}\bar{K}$ for photon energy 38 eV for different emission angles. The angle of incidence was 75°.

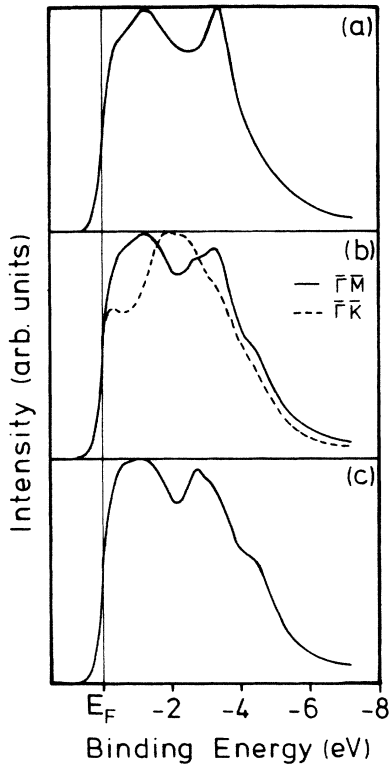

FIG. 7. Theoretical spectra of Ru(001) with photon energy 38 eV and polar angle of emission equal to 10° toward $\bar{\Gamma}\bar{M}$ for both domains [(a) and (c)] and their sum (b) and toward $\bar{\Gamma}\bar{K}$ [dashed line in (b)].

(point of inflection) in the secondary-electron distribution, which marks the bottom of the final-state band (see Fig. 2), in fair agreement with Himpsel *et al.*[7] The critical point at 30 eV and at Γ is determined from the intensity maxima (corrected for monochromator flux) of the −5.4- and −7.3-eV bands (see Fig. 8). Here a 2-eV energy difference with respect to the value of Himpsel *et al.*,[7] exists, which can be attributed to the difficulties in determining the photon energy giving the maximum intensity for the peak with $E_B = -7.3$ eV. The critical point at A with energy 18 eV can be obtained from the behavior of the emission from the upper Δ_2 band. In the spectrum with $h\nu = 20$ eV we can still resolve two peaks near −2.5 eV, whereas with $h\nu = 21$ eV there is only one broad structure to be seen. So assuming that at a photon energy of 20.5 eV we have emission from the A point in k space at energy −2.5 eV, we obtain a critical point around 18 eV. An additional critical point at high energy can be found at $E_K \approx 55$–60 eV. This critical point can most reliably be determined from the intensity ratio of band 2 and the 5.4-eV peak, yielding $E_K \approx 58$ eV, in good agreement with Ref. 7. We place this point at Γ.

There are other critical points found by Himpsel *et al.*[7] Firstly, they have critical points linked with the $E_K = 16.5$ eV final-state structure. The difficulty with these structures is that there is no reasonable way to determine $k_\perp$ and thus we have omitted these points. Then we have the intensity maximum of the 0.3-eV peak at a photon energy of 24 eV. Our interpretation of the origin of this spectral structure differs from that by Himpsel *et al.*[7] This "tail" structure has a maximum intensity when the bands *above* the Fermi level are at the nearest energy to the Fermi level, but the situation may be complicated by the energy dependence of the intensity of these transitions (see discussion below). So we do not consider this structure as an acceptable critical point. Furthermore, Himpsel *et al.*[7]

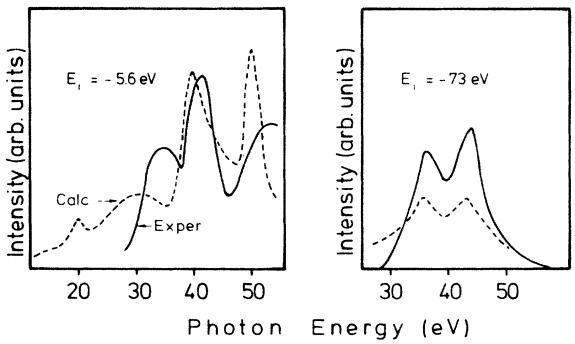

FIG. 8. Intensity of the initial-state peaks at $E_B = \approx -5.6$ eV and the ≈ -7.3-eV peak as a function of photon energy. The dashed curve is the result of the photoemission calculations for the lowest occupied bands.

introduce two critical points to be obtained from a knowledge of the band structure. There are two bands, Δ_2 and Δ_6, which cross the Fermi level, and from an $E_B(h\nu)$ plot we might estimate the crossing photon energy. The necessary $k_\perp$ value is obtained from consideration of the band structure. Our band structure gives $k_\perp$ values of 0.36 and 0.76 in units of $\Gamma A \Gamma$, to be compared with values of 0.36 and 0.80 from Himpsel *et al.*[7] We extrapolate our experimental photon energy for the Δ_2 crossing and obtain a value of $h\nu=12$ eV, in fair agreement with the value of Himpsel *et al.*[7] On the other hand, our data do not allow us to accurately determine the photon energy which corresponds to the crossing of Δ_6. We see a peak at $h\nu=28$ eV, when $E_B=-1.0$ eV. The -0.3-eV structure has maximum intensity at $h\nu=27$ eV, so we could claim that crossing takes place at $h\nu\approx 26$ eV. This value differs by 7 eV from that of Himpsel *et al.*[7] Our value of this doubtful critical point fits nicely into our theoretical complex final-state bands (displayed by dotted lines in Fig. 1), but does not fit into free-electron-like bands.

When we adjust our free-electron-like final-state parabola to these critical points above we derive our experimental inner potential $V_{0,e}=0.0$ eV with respect to the Fermi level, or -5.4 eV with respect to the vacuum level. So our free-electron-like final states are 2 eV above the states determined by Himpsel *et al.*,[7] which leads to a 7.5% difference in $k_\perp$ at $E=20$ eV. Our free-electron-like energy bands are shown in Fig. 1 by dotted lines.

VI. MULTIELECTRON EXCITATIONS

As shown in Fig. 8(b), the peak at -7.3 eV binding energy is resonantly enhanced at the Ru $4p$ core-level thresholds which are at $h\nu=43$ eV ($4p_{3/2}$) and $h\nu=46$ eV ($4p_{1/2}$), respectively. This suggests it to be caused by a two-hole final state. Resonant satellites have first been found for Ni (Ref. 31), and subsequently in many other transition metals.[32,33] There have been intense theoretical and experimental efforts in understanding these two-electron resonances, which are, e.g., reviewed in Ref. 33. In an atomic picture these two-electron resonances can be regarded as super-Coster-Kronig transitions following the $4p\rightarrow 4d$ photoabsorption. The two-electron resonance for Ru at -7.3 eV is of substantial intensity (see Figs. 2, 8, and 9). Experimentally, we see two intensity maxima for the peak at this energy. The first maximum appears at a photon energy of 36 eV. This maximum can be explained by a direct interband transition from the bottom of the valence band, i.e., by a *one*-electron feature. The second maximum appears above the core-level—threshold energies around $h\nu=44$ eV, suggesting multielectron origin. The multielectron excitation is not suppressed by adsorption of CO or H_2, in agreement with expectation. This rules out the possibility that the missing of the resonance in the work of Himpsel *et al.*,[7] can be explained by adsorbed impurities.

Note that our one-electron theory produces a weak peak also at photon energy of 44 eV. This means that even this peak might not be due to multielectron excitations alone. Its strong intensity at the core-level energies, however, favors the predominance of multielectron nature in this range.

The satellite structures are known to be correlated with the d-band width.[1,4] The normal one-electron excitation spectrum is thought to be pushed upward in such a way that the center of gravity of all excitations is conserved. As a consequence, the one-electron d-band spectrum should be narrowed since the top of the nearly filled d bands is pinned at E_F. Himpsel *et al.* estimated this effect to be less than 10% for Ru (Ref. 34). We believe that the Ru band-structure calculations are not accurate enough to discuss this effect in detail.

VII. TWO-DIMENSIONAL STATES

Surface states (or resonances) are identified experimentally by the following criteria: (i) they are sensitive to submonolayer amounts of adsorbates, (ii) they are in a (relative) gap of the bulk band structure, and (iii) as two-dimensional states they are solely dependent on $\mathbf{k}_{||}$ and show no dispersion with $k_\perp$. If the energies of a suspected surface state or resonance are plotted versus $k_\perp$ for various photon energies, the two-dimensional origin can be verified. The cross section of a surface state will vary due to the modulation of the surface-state charge density normal to the surface, even though the surface state is two-dimensional.[35]

In our theoretical intensity calculation we can identify emission from a surface state according to the following criteria: (i) It is excited only by A_z. (ii) The energy of the spectral feature lies in a gap of the bulk band structure. (iii) The energy position should be sensitive to the position of the surface barrier (or to the position of the first atomic layer with respect to the other layers). This behavior is indeed observed with the PEOVER program, as noted before by Larsson[12] and Lindroos.[36] Feibelman[20] also reports such a spacing dependence of surface band position for Rh. (iv) the intensity contribution of the first layer (surface barrier) in the PEOVER program should have a peak. The last is a necessary condition for surface-state emission, but it is not always sufficient. All this concerns only Shockley-type surface states, which are "automatically" reproduced by the PEOVER. When we want to produce Tamm-type surface states by changing the potential of the outermost atomic layer, we can use point (iii) to further identify our peaks. In this study we did not use any tricks to produce peaks for Tamm-type surface states.

According to the band structure of Ru there is a band gap in the vicinity of Γ between -2.9 and -5.5 eV (see Fig. 1). Experimentally, we have a pronounced peak at -5.6 eV with photon energies above 30 eV. In most spectra this structure is, however, rather broad and weak and the exact determination of its energy and its origin is difficult. In other words, at least part of the intensity of this spectral structure could originate from above the Δ_2 band edge. A surface state above the Δ_2 band has been predicted in both available theoretical surface band-structure calculations.[19,20] Also, Himpsel *et al.*[7] and Heskett *et al.*[10] have interpreted the experimental -5.6-eV structure as originating from a surface state. However, this peak is only partly affected by adsorption (see, e.g., Fig. 2 of Heskett *et al.*[10]), which contradicts the experimental criterion (i) for surface states.

To clarify the origin of the −5.6-eV peak we have performed several theoretical intensity calculations. We did these calculations using an arbitrarily small imaginary part of the optical potential, with a value equal to 50 meV. In Fig. 9 we show the intensity of the −5.6-eV peak as a function of photon energy. When the photon energy is increased above $h\nu=34$ eV, the −5.6-eV peak clearly splits into two peaks. The lower peak starts to follow the Δ_1 band dispersion. At $h\nu=44$ eV we see convincingly *three peaks,* two corresponding to direct transitions from Δ_1 and Δ_2. The uppermost peak is the most likely candidate for a surface-state emission. We have changed the position of the surface barrier to test criterion (iii) for the identification of the theoretical surface state. The results are presented in Fig. 10. As can be seen, there is a small but existing shift in the energy position of the uppermost peak at $E=-5.3$ eV. Thus we can conclude that in our theoretical calculations the peak at −5.3 eV originates from a Shockley-type surface state. Experimentally, we cannot resolve these three peaks and we always have surface state and Δ_2 emission mixed together. Furthermore, the experimental spectrum at $h\nu=44$ eV is complicated by the existence of the multielectron peak at −7.3 eV, whose energy coincides with the bottom of the valence band.

A relative gap lies between Δ_5 and Δ_6 at Γ. According to our results this energy gap at $\bar{\Gamma}$ is smaller (≈ -1.3 to −1.9 eV) than the one reported by Himpsel *et al.*,[7] Holzwarth *et al.*[19] have predicted a surface resonance in this energy range. Our experimental and theoretical results are not in agreement with their results and interpretations, since we find no two-dimensional state in this $E(k)$ region. A further energy gap, according to our theory (see Fig. 1), is above the Fermi level between 1.4 and 11 eV. As we can see in Fig. 10, a peak at 2.8 eV also fulfills condition (iii) for a theoretical surface state. Feibelman[20] has predicted such a surface state at ≈ 1 eV above the Fermi level. By changing the distance between surface barrier and the outermost atomic layer from 0.5 times d_z to 0.7 times d_z (d_z is the distance between bulk atomic layers), this surface state is shifted to an energy of 1.4 eV, which is the uppermost energy of the Δ_2 band at

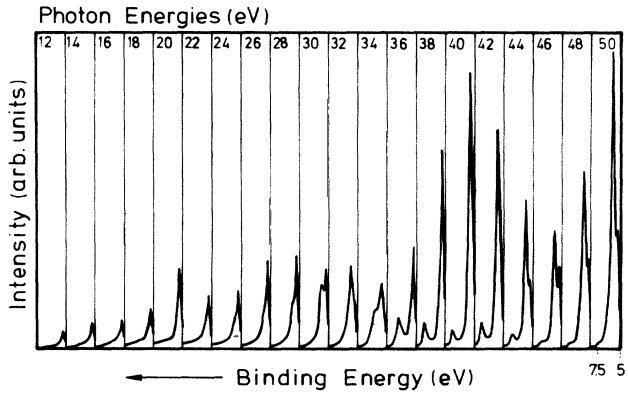

FIG. 9. Theoretical "−5.6-eV" peak calculated with different photon energies for E_B between −7.5 and −5.0 eV (see text).

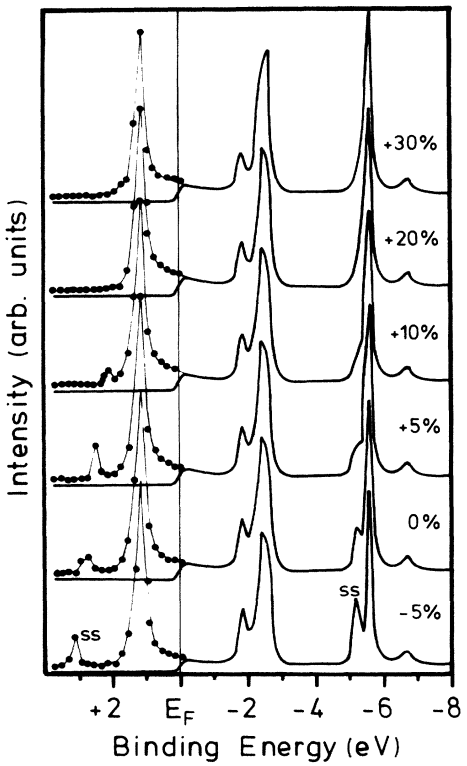

FIG. 10. Theoretical normal-emission spectra of Ru(001) at $h\nu=44$ eV calculated with different positions of the surface barrier. Dotted lines display spectra without taking into account the Fermi distribution of Eq. (11). SS marks the surface state.

Γ. In experiments a tail of the peak originating from this surface-state peak might extend below the Fermi level. The observed intensity decrease of the −0.3-eV peak after adsorption of some impurity gas might be due to disappearance of this surface state above the Fermi level. The other explanation of the intensity decrease might be that bonding of adsorbates induces small changes in the band structure near the Fermi level. Even a small shift of the bands induces large changes in intensity. Experimentally, the −0.3-eV peak shows a $E(k)$ dispersion independent of $h\nu$, as shown in Fig. 14.

Away from $\bar{\Gamma}$ other surface states might exist which are not covered by our present theoretical study, which has been performed for normal emission only. In fact, Fig. 11 indicates a possible surface state around the $\bar{K}$ point at −2 eV. This may be compared to a surface band-structure calculation by Feibelman,[20] which predicts surface states in this $E(\mathbf{k}_{\|})$ region (thick solid lines in Fig. 11).

VIII. COMPARISON BETWEEN EXPERIMENTAL AND THEORETICAL BAND STRUCTURES

Earlier band-structure calculations[8,9,17] have been extended only a few electron volts above the Fermi level. In the interpretation of photoemission spectra we usually need some information on the final-state bands. Bross and Krieter[18] have extended their MAPW calculations up

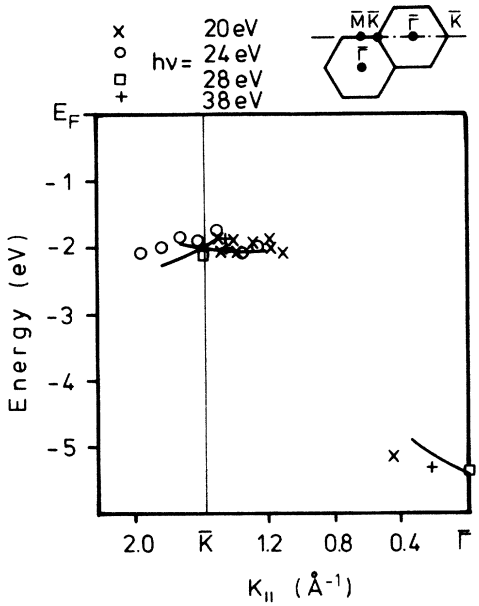

FIG. 11. Two-dimensional band structure of Ru(001) along $\bar{\Gamma}\bar{K}$. Solid lines show theoretical bands from Ref. 20, and symbols are experimental points.

to 20 eV above E_F. Since our experimental data go up to $h\nu=80$ eV, we have extended our calculations up to 70 eV above E_F. The original potential calculations of Moruzzi *et al.*[19] have been performed utilizing the fcc crystal structure. When we used the same crystal structure our results agreed well with their band structure. On the other hand, since the fcc band structure for ΓL deviates so much from the hcp $\Gamma A\Gamma$ structure, we found it necessary to use the proper hcp crystal structure in our calculations (see Fig. 12). The arrangement of energy bands around -2.4 eV confirms the hexagonal crystal structure. The symmetry of the probed initial-state bands was determined by varying the angle of incidence of the incoming polarized light as explained above.

Roughly speaking, all band structures calculated with *proper hcp symmetry* agree reasonably well. The main difference between various theoretical results, as shown in Fig. 13, seems to be the energy position of the lowest band

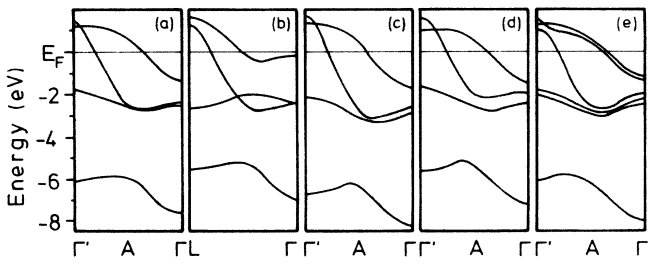

FIG. 12. Comparison of the calculated initial-state energy bands of Ru along $\Gamma A\Gamma$. (a) After Holzwarth and Chelikowsky (Ref. 19). (b) After Moruzzi *et al.* (Ref. 9). (c) After Alekseyev *et al.* (Ref. 17). (d) After Bross and Krieter (Ref. 18). (The result of our calculation is essentially identical; also see Fig. 14.) (e) After Jepsen *et al.* (Ref. 8).

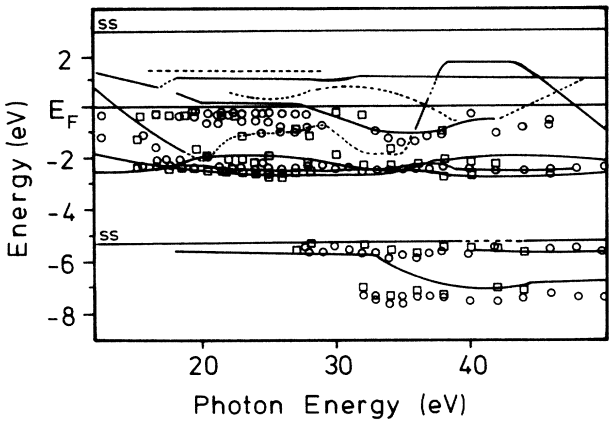

FIG. 13. Experimental (circles) and theoretical (solid lines) $E_B(h\nu)$ plots. Dashed lines refer to the theoretical peaks due to indirect transitions. SS refers to surface state.

and the bottom of the valence band. Our (and also those of Bross) results locate the bottom at -7.0 eV. Holzwarth *et al.*[19] locate it at -7.7 eV and others[8,17] at ≈ -8.0 eV. Our experimental estimate for the bottom of the valence band is -7.3 eV, detectable at a photon energy of 37 eV.

To compare theoretical and experimental results, we show in Fig. 13 a combined $E_B(h\nu)$ plot. Experimental

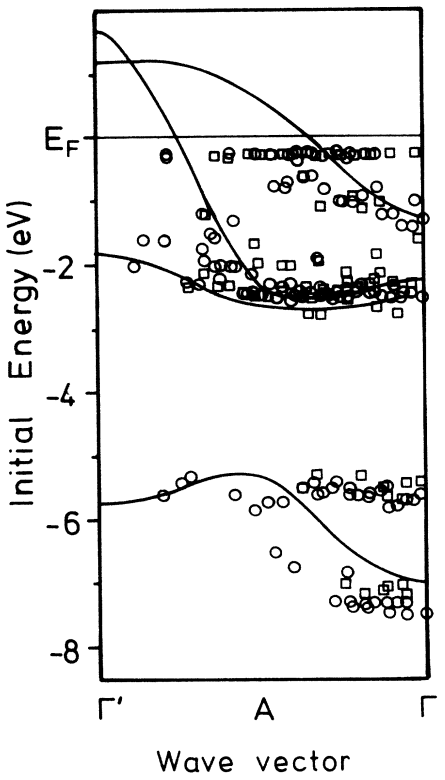

FIG. 14. Experimental band structure of Ru for occupied bands. Circles are derived from data taken at near grazing incidence ($\alpha=75°$). Squares stand for near normal incidence ($\alpha=20°$). The solid lines are from our band-structure calculation.

peak positions (crosses) and theoretical *peak* positions (solid lines) are plotted in the same picture without any direct assumption about the final-state bands. The theoretical points correspond mainly to the crossings of the complex final-state band (see Fig. 1, dashed line) with the initial-state bands. In addition to the direct transitions, we have the two surface states as discussed in the preceding section. Furthermore, we have a peak structure at $E_B = \approx -1$ eV. This structure cannot be a surface state as it is excited by *s*-polarized light. It is probably due to some secondary-cone emission. From the $E_B(h\nu)$ data we can construct an experimental band structure using the described procedure with free-electron-like final states. The result is shown in Fig. 14 together with our theoretical band structure.

Figures 3, 13, and 14 show, in our opinion, rather good agreement between theory and experiment. In particular, the experimental band dispersions for the upper *d* bands as well as for the *sp* band are well reproduced by theory. The polarization dependence of the lower *d* band close to the Γ point is in agreement with theory (the symmetry point Γ_6 is placed at higher binding energy than Γ_1).

We can also compare calculated photoemission peak intensities to experiment. This is shown in Fig. 8 for the lowest band. We have divided theoretical spectra in Fig. 9 into two parts, one below -5.9 eV and the other above it, and have obtained intensities by summing the values for each part. Theory predicts four intensity maxima, at $\approx$20, 30, 40, and 50 eV, which can be identified in the experiment at 34, 42, and 60 eV, respectively. The experimental maximum at 43 eV of the -7.3-eV peak at Γ is due to the multielectron resonance as discussed above. It has to be mentioned that the PEOVER program usually overestimates the intensity of surface states; thus the presence of the surface state in the -5.6-eV peak makes the above comparison not too accurate.

The lifetimes, from the width of the observed structures, have already been determined by Himpsel *et al.*[7] Their values agree well with the present results; we will therefore not repeat their discussion here.

IX. SUMMARY

We have determined the initial- and final-state band structure of Ru along the threefold axis using angle-resolved photoemission.

(1) There is good agreement between experiment and theory for the initial-state bands, if the correct hcp symmetry is used in the calculations.

(2) A peak near the Fermi level is shown to originate from the "tails" (mainly caused by final-state broadening) of the bands just above the Fermi level.

(3) A peak at -5.6 eV consists of three peaks, two from direct interband transitions (one of them is forbidden by dipole selection rules at most energies) and one from an indirect transition involving surface-state emission.

(4) We find a strong two-electron resonance peak at $E_B = -7.3$ eV hitherto not found for Ru.

(5) The prominent peak in the experimental spectra at a fixed kinetic energy of 16.5 eV is attributed to emission into a flat final band in the appropriate energy region.

ACKNOWLEDGMENTS

We thank W. Braun of BESSY for his support, M. Neumann for the provision of the spectrometer used for this work, H. Bross and F. Krieter for helpful discussions and for permission to use their band-structure calculations prior to publication, and W. Brenig and H. Pfnür for fruitful discussions. One of us (M.L.) is grateful to the Alexander von Humboldt Stiftung for financial support. This project was financially supported by the German Bundesministerium für Forschung und Technologie (BMFT) under Grant No. 05-237-MZ.

*Permanent address: Department of Physics, Tampere University of Technology, P.O. Box 527, SF-33101 Tampere, Finland.

[1]F. J. Himpsel, Appl. Opt. **19**, 3964 (1980).

[2]E. W. Plummer and W. Eberhardt, Adv. Chem. Phys. **49**, 533 (1982).

[3]See, e.g., W. Eberhardt and E. W. Plummer, Phys. Rev. B **21**, 3245 (1980).

[4]See, e.g., E. Dietz and F. J. Himpsel, Solid State Commun. **30**, 235 (1979).

[5]M. Pessa, M. Lindroos, H. Asonen, and N. V. Smith, Phys. Rev. B **25**, 738 (1982).

[6]F. J. Himpsel and D. E. Eastman, Phys. Rev. B **21**, 3207 (1980).

[7]F. J. Himpsel, K. Christmann, P. Heimann, and D. E. Eastman, Phys. Rev. B **23**, 2548 (1981).

[8]O. Jepsen, O. K. Andersen, and A. R. Mackintosh, Phys. Rev. B **12**, 3084 (1975).

[9]V. L. Moruzzi, J. F. Janak, and A. R. Williams, *Calculated Electronic Properties of Metals* (Pergamon, New York, 1978).

[10]D. Heskett, E. W. Plummer, R. A. de Paolo, W. Eberhardt, F. M. Hoffmann, and H. R. Moser, Surf. Sci. **164**, 490 (1985).

[11]J. F. L. Hopkinson, J. B. Pendry, and D. J. Titterington, Comput. Phys. Commun. **19**, 69 (1980).

[12]C. G. Larsson, Ph.D. thesis, 1982, Chalmers University of Technology, Göteborg, ISBN-91-7032-078-0 (unpublished).

[13]J. C. Fuggle, T. E. Madey, M. Steinkilberg, and D. Menzel, Surf. Sci. **52**, 521 (1975); E. Umbach and D. Menzel, Chem. Phys. Lett. **84**, 491 (1981); E. Umbach, S. Kulkarni, P. Feulner, and D. Menzel, Surf. Sci. **88**, 65 (1979).

[14]P. Hofmann, A. Zartner, J. Gossler, M. Glanz, and D. Menzel, Surf. Sci. **161**, 303 (1985).

[15]P. Hofmann and D. Menzel, Surf. Sci. **152-153**, 382 (1985).

[16]M. Lindroos, Surf. Sci. **152-153**, 222 (1985).

[17]E. S. Alekseyev, V. A. Ventsel, O. A. Voronov, A. I. Likhter, and M. V. Magnitskaya, Zh. Eksp. Teor. Fiz. **76**, 215 (1979) [Sov. Phys.—JETP **49**, 110 (1979)].
[18]H. Bross and F. Krieter (unpublished). F. Krieter, Diplomarbeit, Universität München, 1984.
[19]N. A. W. Holzwarth and J. R. Chelikowsky, Solid State Commun. **53**, 171 (1985).
[20]P. J. Feibelman, Phys. Rev. B **26**, 5347 (1982).
[21]C. G. Larsson, Surf. Sci. **152-153**, 213 (1985).
[22]W. Braun and G. Jäkisch, in Proceedings of the VIIth International Conference on Vacuum Ultraviolet Radiation Physics, Jerusalem, Israel, 1983 [Ann. Isr. Phys. Soc. **6**, 30 (1983)].
[23]C. Caroli, D. Lederer-Rozenblatt, B. Roulet, and D. Saint-James, Phys. Rev. B **8**, 4552 (1973).
[24]J. B. Pendry, Surf. Sci. **57**, 679 (1976).
[25]M. Lindroos, H. Pfnür, and D. Menzel, **33**, 6684 (1986).
[26]M. S. Chung and T. E. Everhart, J. Appl. Phys. **45**, 707 (1974).
[27]R. Hesse, P. Staib, and D. Menzel, Appl. Phys. **18**, 227 (1979).
[28]R. F. Willis and N. E. Christensen, Phys. Rev. **18**, 5140 (1978).
[29]F. J. Himpsel and D. E. Eastman, Phys. Rev. B **18**, 5236 (1978).
[30]C. G. Olson, D. W. Lynch, and R. Rosei, Phys. Rev. B **22**, 593 (1980); P. S. Wehner, R. S. Williams, S. D. Kevan, D. Denley and D. A. Shirley, *ibid.* **19**, 6164 (1979).
[31]C. Guillot, Y. Ballu, J. Paigné, J. Lecante, K. P. Jain, P. Thiry, R. Pinchaux, Y. Pétroff, and L. M. Falicov, Phys. Rev. Lett. **39**, 1632 (1977).
[32]R. Clauberg, W. Gudat, E. Kisker, E. Kuhlmann, and G. M. Rothenberg, Phys. Rev. Lett. **47**, 1314 (1981).
[33]S. J. Oh, J. W. Allen, I. Lindan, and J. C. Mikkelsen, Jr., Phys. Rev. B **26**, 4845 (1982).
[34]F. J. Himpsel, P. Heimann, and D. E. Eastman, J. Appl. Phys. **52**, 1658 (1981).
[35]P. Hofmann, and K. Kambe, Phys. Rev. B **30**, 3028 (1984).
[36]M. Lindroos, Research Report of Tampere University of Technology, Physics, No. 3, 1982, ISBN-951-720-676-3 (unpublished).